

Classification of Large Cellular Populations and Discovery of Rare Cells Using Single Cell Matrix-Assisted Laser Desorption/Ionization Time-of-Flight Mass Spectrometry

Ta-Hsuan Ong, David J. Kissick, Erik T. Jansson, Troy J. Comi, Elena V. Romanova, Stanislav S. Rubakhin, and Jonathan V. Sweedler*

Department of Chemistry and the Beckman Institute, University of Illinois at Urbana-Champaign, Urbana, Illinois 61801, United States

SUPPORTING INFORMATION

Table of Contents

S-1. Additional Experimental Methods	S-2
S-2. Validating Single Cell Analysis using Neurons from <i>Aplysia californica</i>	S-3
S-3. Details of the Python Script for PCA and PCA-based Outlier Detection	S-4
S-3. Supplementary Figures	S1–S7
S-4. Supplementary Tables	S1–S2

1. Additional Experimental Methods

***Aplysia californica*.** We used a population of larger *Aplysia* neurons to validate our ability to target the center of cells and determine the efficacy of our integrated cell localization and acquisition approaches. Details on these experiments are provided here.

Sample Preparation. Adult *A. californica* (175–250 g; National Resource for Aplysia, Rosenstiel School of Marine & Atmospheric Science, Miami, FL) were kept in an aquarium containing continuously circulated and aerated seawater made using Instant Ocean Aquarium Sea Salt Mixture (<http://www.instantocean.com>, accessed – 05/26/14), maintained at 14 °C. The central nervous system (CNS) was surgically isolated after animal anesthesia with isotonic MgCl₂ solution injected into the body cavity. The CNS tissue was placed in artificial sea water (ASW) composed of 460 mM NaCl, 10 mM KCl, 10 mM CaCl₂, 22 mM MgCl₂, 26 mM MgSO₄ and 10 mM HEPES in Milli-Q water (Milli-Q filtration system; Millipore, Billerica, MA), with the pH adjusted to 7.8 using 1 M NaOH in Milli-Q water. Multiple neurons were mechanically isolated from the pleural and pedal ganglia after treatment with freshly prepared 1% (wt/vol) protease type IX dissolved in ASW supplemented with 100 units/mL penicillin G, 100 µg/mL streptomycin and 100 µg/mL gentamicin. The neurons were stabilized in a solution containing 33% glycerol and 67% ASW (v/v) and dispersed onto indium tin oxide-coated glass slides. Excess extracellular glycerol was removed with a water rinse. Roughly 30 *Aplysia* neurons from the sample slide were randomly chosen for analysis.

MALDI TOF-MS. *Aplysia* neurons were used to validate our ability to target single cells. The MALDI matrix α -cyano-4-hydroxycinnamic acid (CHCA) was sublimed onto the *Aplysia* neuron sample slide to create a uniform matrix layer that is easy to ablate with the MALDI laser. Sublimation was done in a glass sublimation chamber (Ace Glass, Vineland, NJ), heated with a heating mantle powered using a variable autotransformer set to 55% of 120 V (Staco Energy Products Co., Dayton, OH). A vacuum was created using an Edwards 30 E2M30 rotary pump (Edwards, Sanborn, NY). The setup was run for 18.5 min to create a coating of ~0.2 mg/cm². A population of ~30 *Aplysia* neurons was profiled with a 3 × 3 spot array at each cell with 90 µm raster using 1000 laser shots fired at 1000 Hz using a Bruker ultrafleXtreme mass spectrometer (Bruker Daltonics, Billerica, MA). The laser spot size was set to “small” with a diameter of ~30 µm.

Pituitary Peptide Characterization via LC–MS. In order to identify the peptides detected in the individual cell pituitary spectra, we extracted peptides from larger samples and characterized them using two distinct LC–MS systems.

Extraction. Peptide extraction was conducted on two types of pituitary samples. To identify the unknown ion observed at m/z 2105.3, a suspension (100 µL) of dissociated rat anterior pituitary cells was homogenized in 200 µL of 10 mM HCl (Avantor, Center Valley, PA). The homogenate was centrifuged (Eppendorf, Hauppauge, NY) at ~21,000 g for 15 min at 4 °C. An aliquot (150 µL) of the supernatant was desalted using a C18 spin column (Thermo Scientific, Waltham, MA). The column was washed twice using 200 µL of 5% acetonitrile (ACN) and 0.1% formic acid (FA). Retained peptides were eluted with two volumes of 40 µL of 50% ACN and 0.1% FA, followed by two volumes of 40 µL of 70% ACN and 0.1% FA. The combined eluent was dried and reconstituted in 10 µL of 0.1% FA. To confirm other peptide markers, rat posterior and intermediate pituitary tissues were homogenized in 200 µL of 10 mM HCl and centrifuged at ~21,000 × g for 15 min at 4 °C. The extract was analyzed with tandem MS (MS/MS) using the Bruker ultrafleXtreme mass spectrometer.

Capillary liquid chromatography (capLC)–MALDI MS/MS. Extract from dissociated rat anterior pituitary was subjected to capLC–MS analysis to identify the unknown ion at m/z 2105.3. High performance LC separation was conducted using a Dionex UltiMate 3000 Rapid Separation system (Thermo Scientific) equipped with a desalting/pre-concentrating setup and a UV detector. Samples were loaded onto a peptide trap column (Acclaim PepMap C18, 200-µm inner diameter (i.d.) × 2 cm, 5-µm particles, 100 Å pore size, Thermo Scientific) and washed for 5 min with a solution of 4% ACN and 0.05% FA. The peptide trap was then placed in-line with the analytical column and separation was conducted on a reversed phase capillary column (Acclaim PepMap

RSLC, C18, 300- μm i.d. \times 15 cm, 2 μm -particle size, 100 \AA pore size, Thermo Scientific). A total of 6 μL of the extract was separated at a uniform flow rate of 4 $\mu\text{L}/\text{min}$ and a gradient of 4–55% solvent B (80% ACN, 0.05% FA, 0.001% trifluoroacetic acid) over 35 min; the entire run time was 60 min at 45 $^{\circ}\text{C}$. Solvent A was 0.05% FA. Separation was monitored with a UV detector at 214 nm. LC fractions were automatically spotted onto a steel MALDI target plate pre-coated with 2,5-dihydroxybenzoic acid (1 mg/cm^2 coating thickness applied via pneumatic spray) at 15 s intervals using a Proteiner fc fraction collector (Bruker Daltonics). Spots were profiled using the Bruker ultrafleXtreme mass spectrometer.

capLC–electrospray ionization (ESI) MS/MS and Bioinformatic Identification of Dissociated Pituitary Peptides. We used 2 μL of the same extract as for the capLC–MALDI MS/MS. Separation was performed at a flow rate of 5 $\mu\text{L}/\text{min}$ and 4–50% gradient B for 70 min at 45 $^{\circ}\text{C}$. MS and MS/MS data were collected on an amaZon speed ETD ion trap mass spectrometer (Bruker Daltonics) interfaced to the LC instrument via a standard ESI source. The parameters included a mass scan range of m/z 300–2800, m/z 4 precursor isolation window, and smart fragmentation for optimized collision energy. Data-dependent precursor selection was restricted to two fragmentation spectra for the top three ions per 0.5 min, and preferred precursor masses (± 0.5), corresponding to the different charge states of m/z 2105, were activated. Base peak chromatograms for MS/MS from each run were processed for peak picking/compound identification, charge deconvolution and retention time-range selection using the dataAnalysis software (Bruker Daltonics) and exported as Mascot generic files (.mgf).

The .mgf files were loaded into PEAKS Studio 5.3 (Bioinformatics Solutions Inc., Waterloo, ON Canada) and processed for charge state correction and *de novo* tag identification. The tags were searched against the rat Uniprot database (<http://www.uniprot.org/>) with 33,475 protein entries. The search parameters included 0.5 Da mass tolerance for precursor and fragment ions, no enzymes, and a maximum of three variable modifications, amidation, acetylation, and pyroglutamylation (from Q and E, disulfide bond formation). The false-discovery rate for peptide-spectrum match was 3.2%, and the average local confidence score for *de novo* sequencing was 50%. Results were filtered with the Peaks peptide score (-10lgP) cutoff of 15, which was chosen according to the histogram of peptide-spectrum match score distribution relative to decoy hits and the plot of precursor mass error *versus* score. Additionally, the filtered results were manually checked for ion fragment/post-translational modification fit to eliminate false-positive identifications. The final peptide lists from the two analyses were combined.

2. Validating Single Cell Analysis using Neurons from *Aplysia californica*

To determine which part of the stretched sample method is amenable to the current approach, a preliminary experiment was conducted on ~ 30 bag cell neurons and pleural sensory neurons from *A. californica*. The goal was to demonstrate sufficient visualization and targeting accuracy for cellular features. The primary modification to the prior method was the optical imaging step. Although brightfield imaging was sufficient previously, it did not produce adequate image contrast for the variety of cell types and experimental conditions in this study. Without cellular labeling, a complex imaging set up was necessary to clearly visualize cells. In the case of the *Aplysia* neurons, autofluorescence and darkfield images were acquired. Cells were visualized as pink spots by restricting darkfield imaging to the red channel of the microscope camera and autofluorescence to the blue channel (Figure S1). To visualize targeting accuracy, the MALDI matrix CHCA was sublimed onto the slide to create a homogeneous coating, and cell locations were ablated using the MALDI laser.

Figure S1 shows an overlay of two optical images taken before and after matrix ablation. The top layer is the pre-ablation darkfield and autofluorescence image. The bottom layer is a brightfield image showing laser ablated spots in the matrix. For these relatively large cells, a 3 \times 3 raster was used for each targeted location. There is good registry between the cells and ablated spots, demonstrating sufficient targeting accuracy. While encouraging, Figure S1 also shows the potential to co-analyze cell clusters and other debris along with single cells. These unwanted features can be removed by setting the boundaries for size and circularity in the “analyze particles” function in ImageJ during cell finding. For example, an upper limit on particle size can be used to exclude cell clusters (Figure S2).

3. Details of the Python Script for PCA and PCA-based Outlier Detection

The script (provided as an additional Supporting Information file, `Principal_Component_Outlier_Analysis_and_Visualization.txt`) operates in the Windows operating system and was written for Python 3.3 (www.python.org). The script is provided as a text file with a `.txt` file extension for easy access. It can be changed to a python script file by changing the `.txt` file extension to a `.py` file extension without modifying the code. It requires the modules `tkinter`, `itertools`, `re`, `os`, `numpy` `scipy` and `matplotlib` to be installed (these modules are available at www.lfd.uci.edu/~gohlke/pythonlibs/, which contains the unofficial Windows binaries for Python). The script loads Bruker data files in the XMass format generated by flexControl 3.4 (build 135) and delimited text files exported from flexAnalysis 3.4 (build 70). Loading other data formats may require the data reading section to be modified.

When first initialized, the user is prompted to select a data directory, an upper and lower bound for the mass range to analyze, and the number of principal components for outlier analysis. It is possible to edit the script to change the normalization methods (line 138) and to modify the top hat background estimation (line 128).

Once the analysis parameters are set, PCA and PCA-based outlier detection are conducted and three plotting windows are generated. These include (window name in parentheses): the raw data plot and principal component data projection (Raw Spectra and PC Space), outlier spectra and individual spectra compared to the reconstruction error (Outlier and Spectra Plots), and a scatter plot of the locations from which the spectra were acquired (Selected m/z Range Image). The number of principal components used in the outlier detection process can be changed by scrolling over the outlier spectrum. Selecting a range on the outlier spectrum or the data/reconstruction error spectrum changes the color scale of the scatter plot to correspond to the signal intensity of that range. Selecting a point from the scatter plot updates the spectrum and reconstruction error spectrum that is displayed.

3. Supplementary Figures

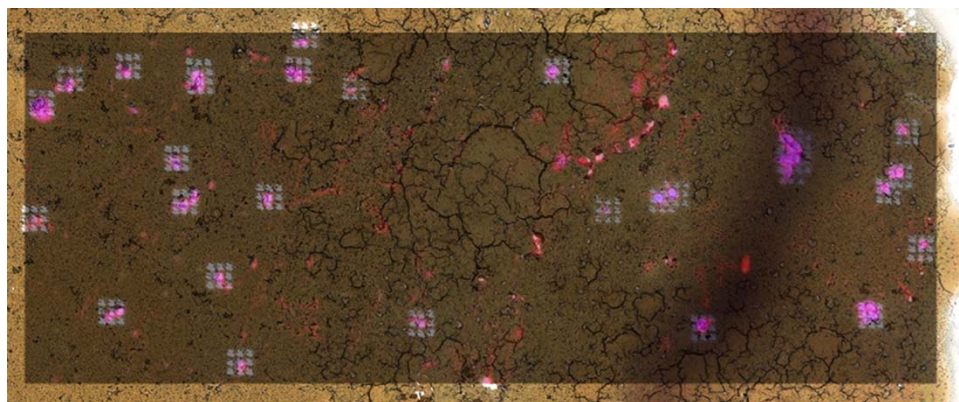


Figure S1. An overlay of two images of dispersed *Aplysia californica* neurons on a microscope slide. The top layer is a combined darkfield and autofluorescence image taken before MALDI matrix application. The bottom layer is a brightfield image of the same sample after matrix application and MALDI-TOF MS analysis. Cells are visualized as pink spots in the darkfield and autofluorescence image. MALDI laser ablation marks (3×3 grids) are visualized as white spots in the matrix layer (gray spots in this overlaid image). There is good registry between cell locations and laser marks, showing our ability to target cells for MALDI MS.

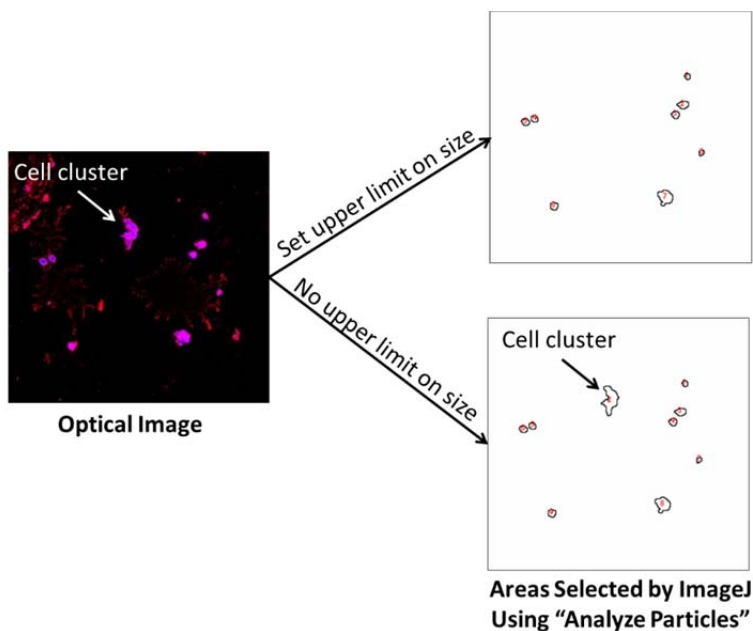


Figure S2. The particle size and circularity settings in the “Analyze Particles” function of ImageJ can be used to remove unwanted features from the analysis. In the case of cell clusters, an upper limit on particle size can be used to exclude them.

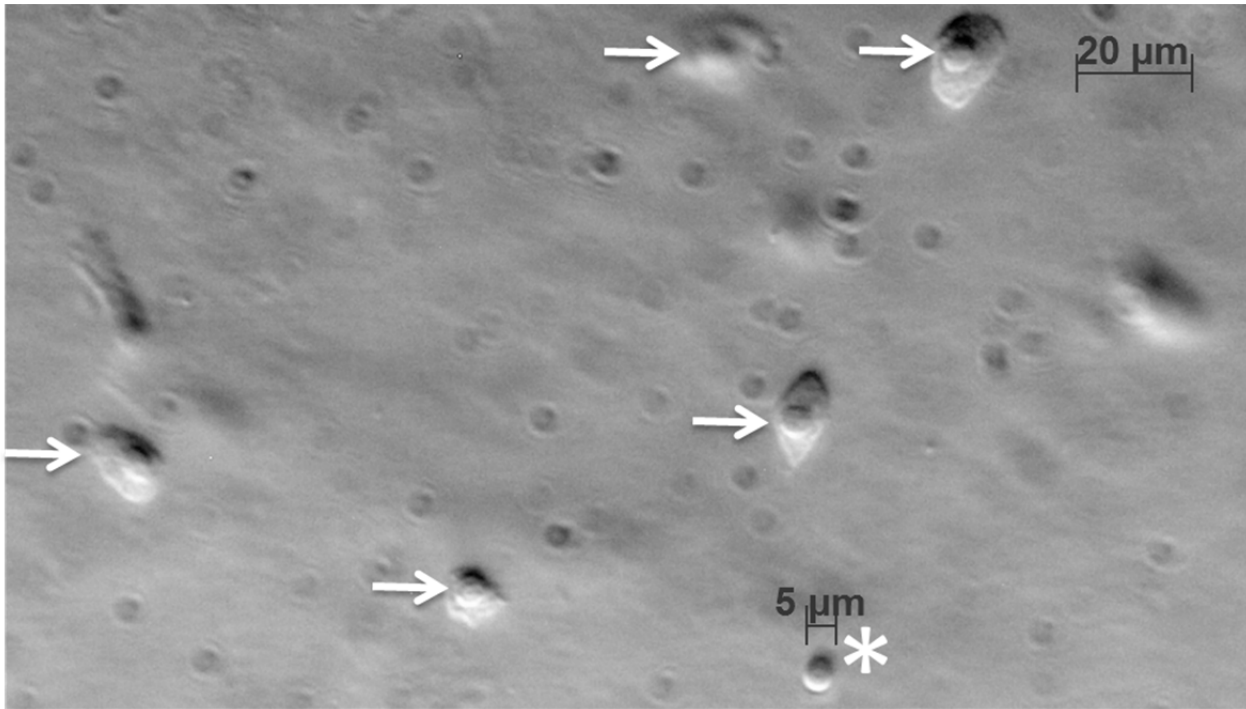


Figure S3. Transmission optical microphotograph of representative cells from enzymatically dissociated rat pituitary. Cells are labeled with arrows and a putative nucleus released from a damaged cell is labeled with an asterisk.

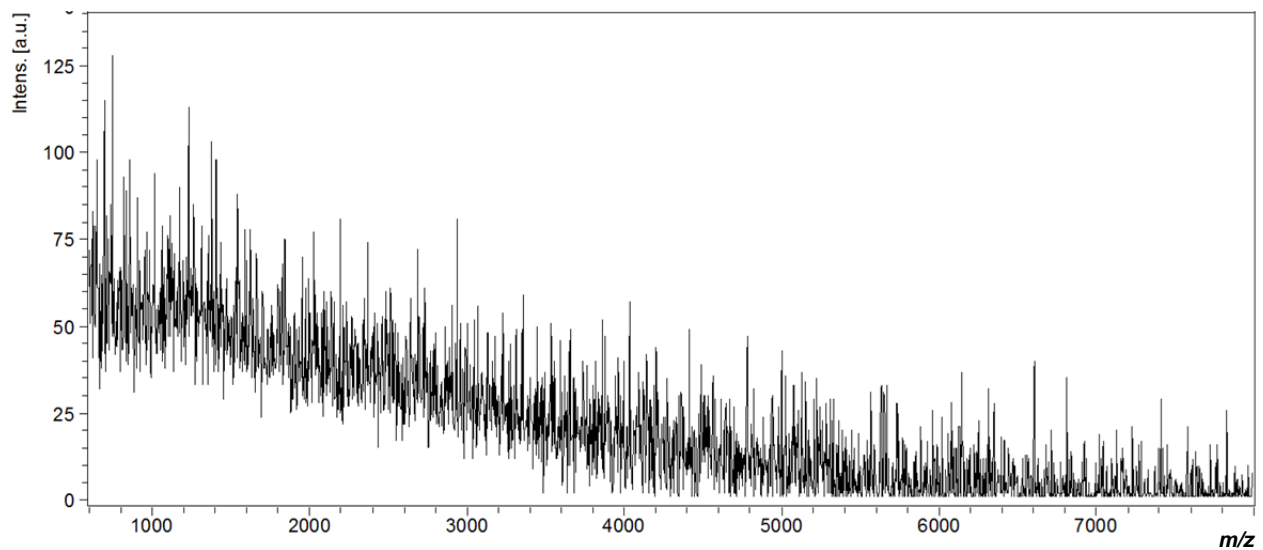
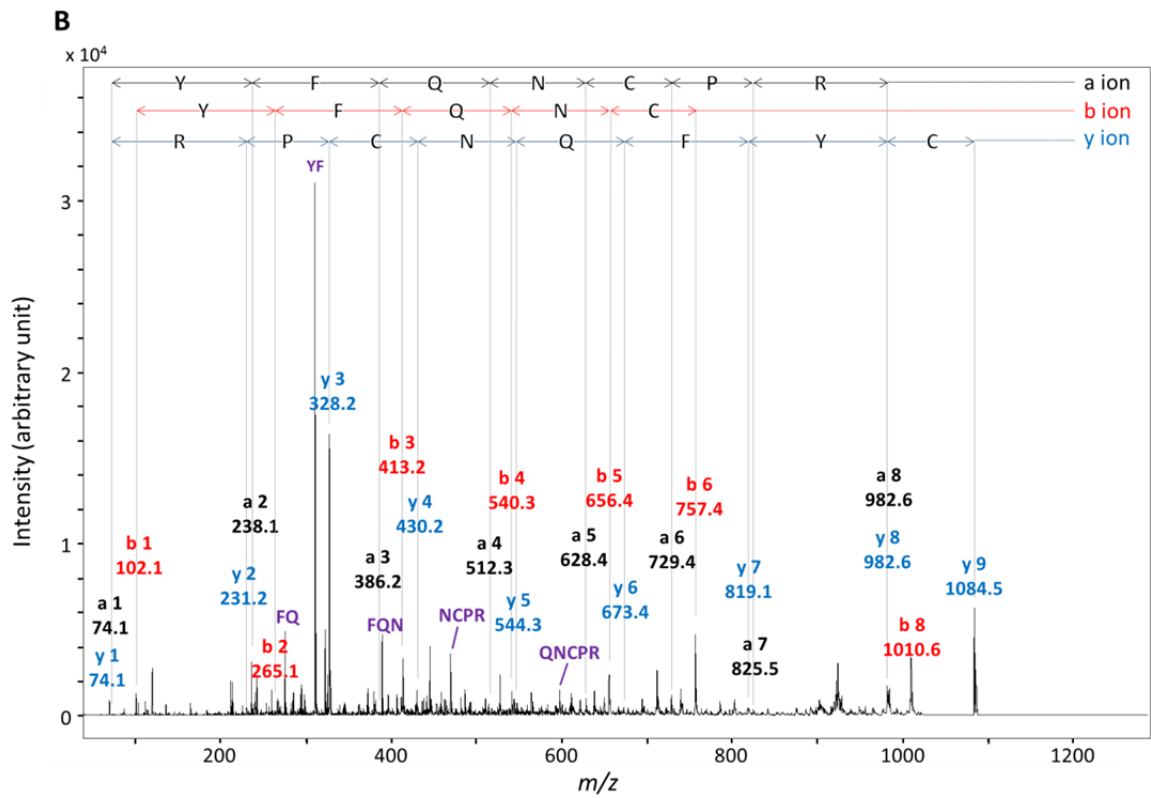
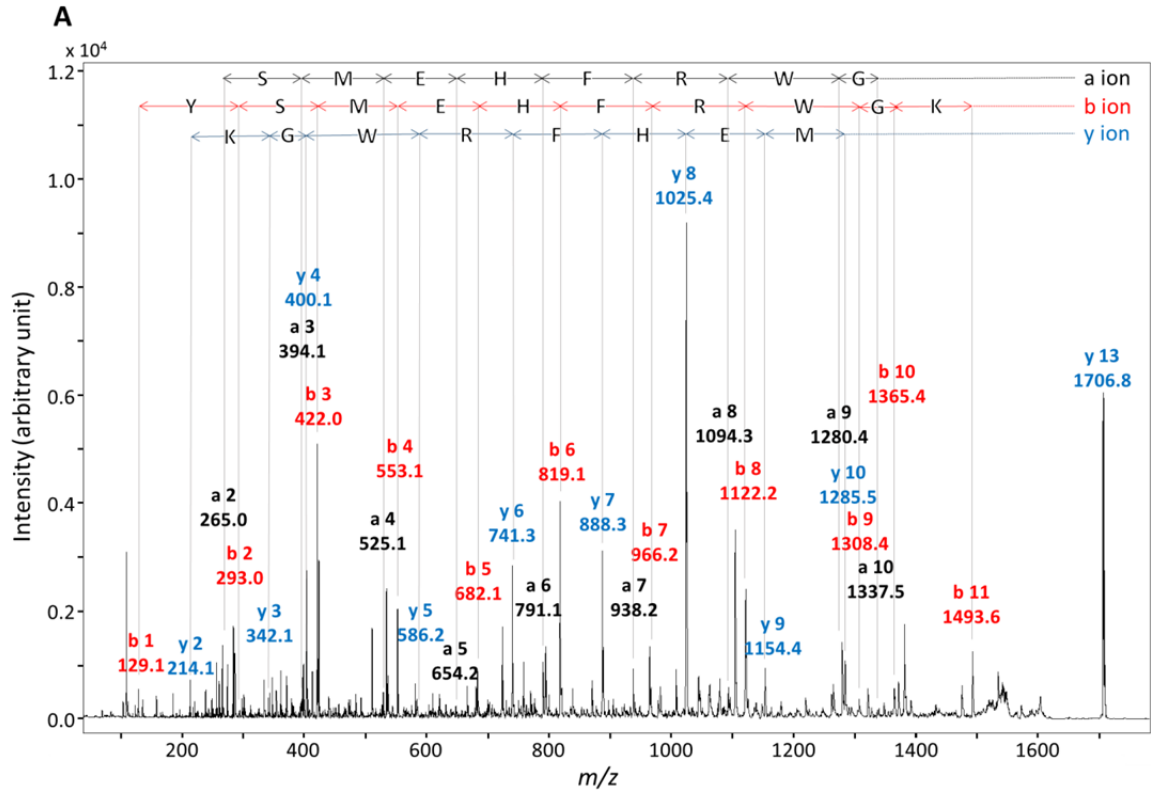


Figure S4. Mass spectrum of a solution containing the nuclear dye Hoechst 33342 from m/z 600–8000. No interfering signals in the analyzed molecular mass range were observed.



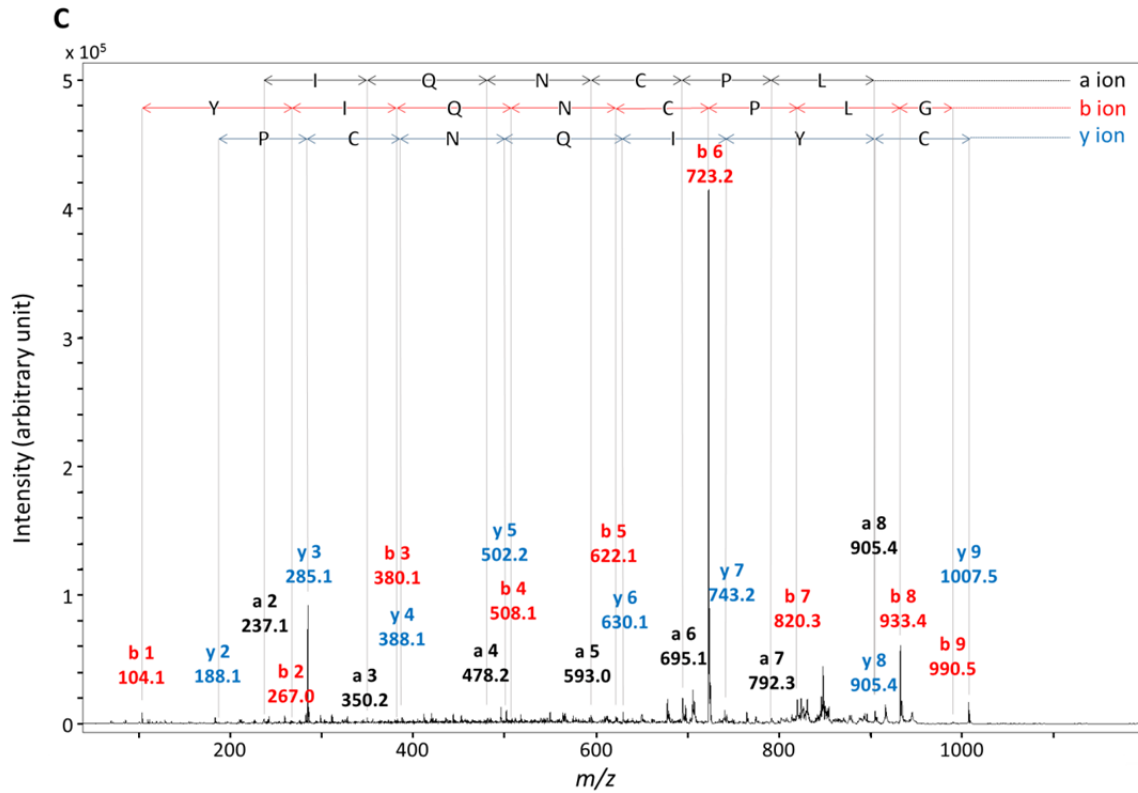


Figure S5. MALDI-TOF MS/MS analysis of peptide markers from intermediate and posterior pituitary extracts. (A) ac- α -MSH (Ac-Ac-SYSMEHFRWGKPV); (B) AVP (CYFQNCPRGa); (C) oxytocin (CYIQNCPLGa).

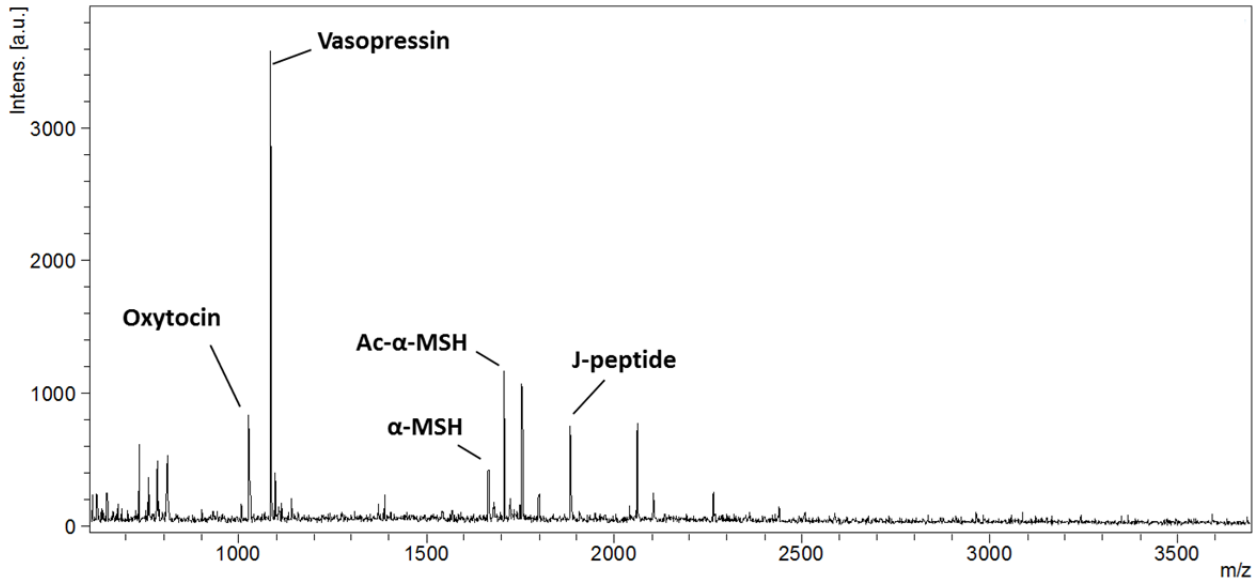
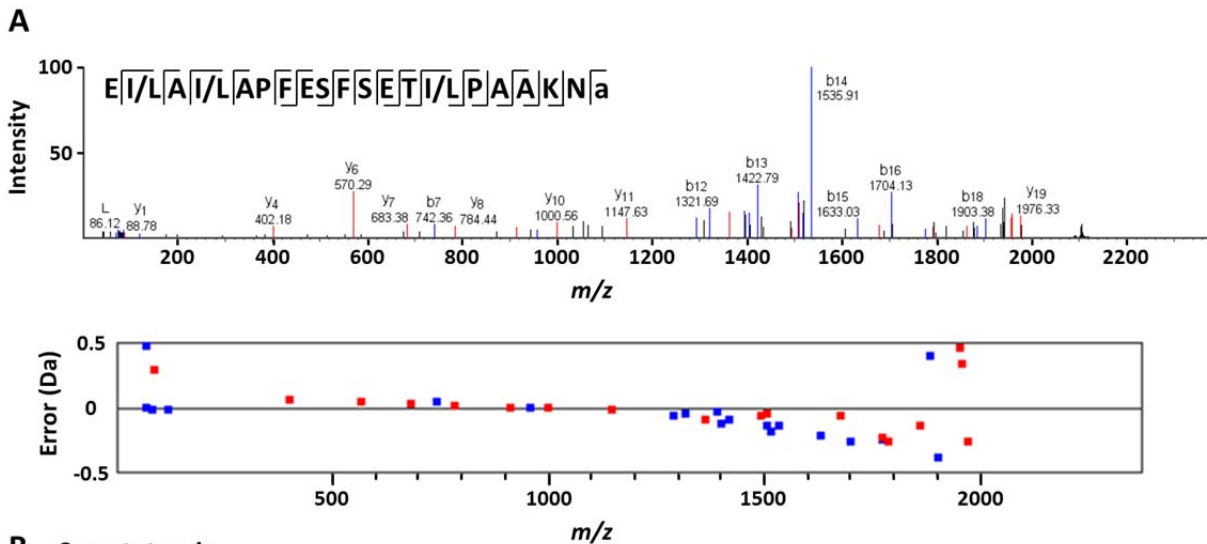


Figure S6. Representative mass spectrum exhibiting AVP, oxytocin, and POMC-derived peptide signals, indicating possible cross contamination between cell types or co-localization of cellular structures, such as presynaptic buttons attached to the examined cells.



B Somatotropin
 MAADSQTPWLLTFSL LCLLWPQEAGAFPAMPLSSLFANAVLRAQHLHQLAADTYKEFERAYIPEGQR
 YSIQNAQA AFC **FSETI PA**PTGKEEAQQRDTMELLRFSLLLIQSWLGPVQFLSRIFTNSLMFGTSDRV
 YEKLKDL EEGIQALMQELEDGSPRIGQILKQTYDKFDANMRSD DALLKNYGLLSCFKDLHKAETYL
 RVMKRRFAESSCAF

Figure S7. MS/MS analysis of an unidentified signal at m/z 2105.3. (A) *De novo* sequencing and mass error for assigned fragments. (B) Sequence for somatotropin in rat. Only a portion of the proposed sequence from *de novo* sequencing is present (red).

4. Supplementary Tables

Table S1. Characteristic ions for major cell populations, including melanotrophs from the intermediate pituitary, AVP-containing and oxytocin-containing cells from the posterior pituitary, and unidentified *m/z* 2105-containing cells.

Melanotroph		AVP-containing		Oxytocin-containing		<i>m/z</i> 2105-containing	
<i>m/z</i> (observed)	Identification	<i>m/z</i> (observed)	Identification	<i>m/z</i> (observed)	Identification	<i>m/z</i> (observed)	Identification
1338.8	amidated, γ -MSH	1084.5	AVP	1007.6	oxytocin (H ⁺)	2104.3	POMC (141-162)
1665.0	amidated, α -MSH			1028.5	oxytocin (Na ⁺)		
1706.9	amidated, acetylated α -MSH						
1883.0	amidated, joining peptide (1-18)						
2506.5	CLIP						
2586.5	phosphorylated CLIP						
2900.8	Ac- β -endorphin (1-26)						
3038.0	Ac- β -endorphin (1-27)						

Table S2. Identified proteins from LC–ESI MS/MS conducted on dissociated rat anterior pituitary cells. Bolded entries include secretogranin, somatotropin and prolactin. Somatotropin and prolactin are expressed in somatotrophs and lactotrophs, respectively, in the anterior pituitary.

Accession	Score (%)	-10lgP	Mass	Description
A1Z0K8 A1Z0K8_RAT	98.7	84.02	31747.42	Beta-actin (Fragment) OS= <i>Rattus norvegicus</i> GN=Actg1 PE=2 SV=1
B0BMT0 B0BMT0_RAT	79.3	47.16	42008.97	RCG47746, isoform CRA_a OS= <i>Rattus norvegicus</i> GN=Acta2 PE=2 SV=1
B1H216 B1H216_RAT	98.4	89.04	15328.52	Hemoglobin alpha, adult chain 2 OS= <i>Rattus norvegicus</i> GN=Hba1 PE=2 SV=1
B2RYR2 B2RYR2_RAT	98.3	101.38	24656.31	Growth hormone OS= <i>Rattus norvegicus</i> GN=Gh1 PE=2 SV=1
B2RYT1 B2RYT1_RAT	99	88.74	25681.52	Prl protein OS= <i>Rattus norvegicus</i> GN=Prl PE=2 SV=1
B5DEM6 B5DEM6_RAT	99	88.74	25752.6	Prolactin OS= <i>Rattus norvegicus</i> GN=Prl PE=2 SV=1
D3Z8J4 D3Z8J4_RAT	53.3	22.82	104957.64	Protein RGD1305422 OS= <i>Rattus norvegicus</i> GN=RGD1305422 PE=2 SV=1
D3ZA47 D3ZA47_RAT	53.3	22.82	106504.43	Protein RGD1305422 OS= <i>Rattus norvegicus</i> GN=RGD1305422 PE=2 SV=1
D3ZLY9 D3ZLY9_RAT	26.3	29.1	13920.16	Histone H2B OS= <i>Rattus norvegicus</i> GN=Hist1h2b1 PE=3 SV=2
D3ZNH4 D3ZNH4_RAT	26.3	29.1	15493.03	Histone H2B OS= <i>Rattus norvegicus</i> GN=Hist1h2bo PE=3 SV=1
D3ZNZ9 D3ZNZ9_RAT	26.3	29.1	13994.2	Histone H2B OS= <i>Rattus norvegicus</i> GN=Hist3h2ba PE=3 SV=1
D3ZWM5 D3ZWM5_RAT	26.3	29.1	13964.21	Histone H2B OS= <i>Rattus norvegicus</i> GN=Hist1h2bb PE=3 SV=2
D4A817 D4A817_RAT	26.3	29.1	13908.15	Histone H2B OS= <i>Rattus norvegicus</i> GN=Hist1h2bh PE=3 SV=2

G3V7X2 G3V7X2_RAT	98.7	85.38	71001.3	Secretogranin 2, isoform CRA_a OS= <i>Rattus norvegicus</i> GN=Scg2 PE=4 SV=1
G3V8B3 G3V8B3_RAT	26.3	29.1	13906.13	Histone H2B OS= <i>Rattus norvegicus</i> GN=LOC684797 PE=3 SV=1
G3V9C7 G3V9C7_RAT	26.3	29.1	13890.13	Histone H2B OS= <i>Rattus norvegicus</i> GN=Hist1h2bk PE=3 SV=1
M0R4L7 M0R4L7_RAT	26.3	29.1	13910.12	Protein Hist1h2bf OS= <i>Rattus norvegicus</i> GN=Hist1h2bf PE=4 SV=1
M0R5B4 M0R5B4_RAT	80.2	56.8	38605.6	Uncharacterized protein OS= <i>Rattus norvegicus</i> PE=4 SV=1
M0R757 M0R757_RAT	95.5	53.04	50107.93	Protein LOC100360413 OS= <i>Rattus norvegicus</i> GN=LOC100360413 PE=4 SV=1
M0R7B4 M0R7B4_RAT	59.3	34.26	23211.92	Protein LOC684828 OS= <i>Rattus norvegicus</i> GN=LOC684828 PE=4 SV=1
M0RAE3 M0RAE3_RAT	53.3	22.82	97773.02	Protein RGD1305422 OS= <i>Rattus norvegicus</i> GN=RGD1305422 PE=4 SV=1
M0RBQ5 M0RBQ5_RAT	26.3	29.1	13908.1	Protein Hist3h2bb OS= <i>Rattus norvegicus</i> GN=Hist3h2bb PE=4 SV=1
Q4KM71 Q4KM71_RAT	50	26.75	75486.94	Splicing factor proline/glutamine rich (Polypyrimidine tract binding protein associated) OS= <i>Rattus norvegicus</i>
Q6P7R4 Q6P7R4_RAT	98.7	85.38	66663.5	Scg2 protein OS= <i>Rattus norvegicus</i> GN=Scg2 PE=2 SV=1
sp A9UMV8 H2AJ_RAT	73	75.88	14045.44	Histone H2A.J OS= <i>Rattus norvegicus</i> GN=H2afj PE=2 SV=1
sp P01237 PRL_RAT	99	88.74	25752.6	Prolactin OS= <i>Rattus norvegicus</i> GN=Pr1 PE=1 SV=1
sp P01244 SOMA_RAT	98.3	101.38	24656.31	Somatotropin OS= <i>Rattus norvegicus</i> GN=Gh1 PE=1 SV=1
sp P01946 HBA_RAT	98.4	89.04	15328.52	Hemoglobin subunit alpha-1/2 OS= <i>Rattus norvegicus</i> GN=Hba1 PE=1 SV=3

sp P02091 HBB1_RAT	98.5	95.41	15979.38	Hemoglobin subunit beta-1 OS= <i>Rattus norvegicus</i> GN=Hbb PE=1 SV=3
sp P02262 H2A1_RAT	73	75.88	14077.44	Histone H2A type 1 OS= <i>Rattus norvegicus</i> PE=1 SV=2
sp P05065 ALDOA_RAT	60.7	36.63	39351.96	Fructose-bisphosphate aldolase A OS= <i>Rattus norvegicus</i> GN=Aldoa PE=1 SV=2
sp P06761 GRP78_RAT	60.3	34.27	72347.09	78 kDa glucose-regulated protein OS= <i>Rattus norvegicus</i> GN=Hspa5 PE=1 SV=1
sp P0C169 H2A1C_RAT	73	75.88	14105.46	Histone H2A type 1-C OS= <i>Rattus norvegicus</i> PE=1 SV=2
sp P0C170 H2A1E_RAT	73	75.88	14119.49	Histone H2A type 1-E OS= <i>Rattus norvegicus</i> PE=1 SV=2
sp P0CC09 H2A2A_RAT	73	75.88	14095.48	Histone H2A type 2-A OS= <i>Rattus norvegicus</i> GN=Hist2h2aa3 PE=1 SV=1
sp P10362 SCG2_RAT	93.8	60.59	71031.33	Secretogranin-2 OS= <i>Rattus norvegicus</i> GN=Scg2 PE=2 SV=1
sp P15865 H14_RAT	81.8	51.29	21987.33	Histone H1.4 OS= <i>Rattus norvegicus</i> GN=Hist1h1e PE=1 SV=3
sp P60711 ACTB_RAT	98.7	84.02	41736.75	Actin, cytoplasmic 1 OS= <i>Rattus norvegicus</i> GN=Actb PE=1 SV=1
sp P61983 1433G_RAT	50.8	26.92	28302.58	14-3-3 protein gamma OS= <i>Rattus norvegicus</i> GN=Ywhag PE=1 SV=2
sp P62630 EF1A1_RAT	95.5	53.04	50113.89	Elongation factor 1-alpha 1 OS= <i>Rattus norvegicus</i> GN=Eef1a1 PE=1 SV=1
sp P62738 ACTA_RAT	79.3	47.16	42008.97	Actin, aortic smooth muscle OS= <i>Rattus norvegicus</i> GN=Acta2 PE=2 SV=1
sp P62804 H4_RAT	85.1	35.22	11367.34	Histone H4 OS= <i>Rattus norvegicus</i> GN=Hist1h4b PE=1 SV=2
sp P63102 1433Z_RAT	60.7	37.14	27771.13	14-3-3 protein zeta/delta OS= <i>Rattus norvegicus</i> GN=Ywhaz PE=1 SV=1
sp P63259 ACTG_RAT	98.7	84.02	41792.86	Actin, cytoplasmic 2 OS= <i>Rattus norvegicus</i> GN=Actg1 PE=1 SV=1

sp P63269 ACTH_RAT	79.3	47.16	41876.9	Actin, gamma-enteric smooth muscle OS= <i>Rattus norvegicus</i> GN=Actg2 PE=2 SV=1
sp P68035 ACTC_RAT	79.3	47.16	42018.99	Actin, alpha cardiac muscle 1 OS= <i>Rattus norvegicus</i> GN=Actc1 PE=2 SV=1
sp P68136 ACTS_RAT	79.3	47.16	42051.05	Actin, alpha skeletal muscle OS= <i>Rattus norvegicus</i> GN=Acta1 PE=1 SV=1
sp P68255 1433T_RAT	50.8	26.92	27778.27	14-3-3 protein theta OS= <i>Rattus norvegicus</i> GN=Ywhaq PE=1 SV=1
sp P68511 1433F_RAT	50.8	26.92	28211.72	14-3-3 protein eta OS= <i>Rattus norvegicus</i> GN=Ywhah PE=1 SV=2
sp Q00715 H2B1_RAT	26.3	29.1	13990.21	Histone H2B type 1 OS= <i>Rattus norvegicus</i> PE=1 SV=2
sp Q00728 H2A4_RAT	73	75.88	14283.6	Histone H2A type 4 OS= <i>Rattus norvegicus</i> PE=2 SV=2
sp Q4FZT6 H2A3_RAT	73	75.88	14121.46	Histone H2A type 3 OS= <i>Rattus norvegicus</i> PE=2 SV=3
sp Q64598 H2A1F_RAT	73	75.88	14175.55	Histone H2A type 1-F OS= <i>Rattus norvegicus</i> PE=3 SV=3